Synthesis and electronic properties of *Ln*RhAsO and *Ln*IrAsO compositions

Sean Muir, A.W. Sleight, M.A. Subramanian*

Department of Chemistry, Oregon State University, Corvallis, OR 97330, USA

ARTICLE INFO

ABSTRACT

The synthesis and characterization of the new compositions LnRhAsO ($Ln=$Ce, Nd) and LnIrAsO ($Ln=$La, Ce, Nd) are reported. These compounds crystallize in the ZrCuSiAs type structure, isostructural to iron pnictide LnFeAsO materials. Upon substitution of Rh for Fe, both a and c lattice parameters increase relative to $3d$ transition metal compounds; however, when Ir is substituted for Rh the a-parameter decreases slightly while the c-parameter expands. The decrease in a lattice parameter corresponds to a short metal–metal distance in Ir compounds. CeRhAsO and CeIrAsO compositions show abrupt decreases in resistivity at 7 and 10 K, respectively, coinciding with a small shift in magnetization at the transition temperature.

1. Introduction

The iron pnictide discoveries have recently sparked a wildfire of superconductor research and rekindled the scientific community's fascination with layered structures [1–6]. Low dimensionality can promote electronic correlation and this is partially why metallic compounds crystallizing in anisotropic structures are known to exhibit many exciting transport properties. LaFeAsO belongs to a large structural family often referred to as ZrCuSiAs type materials [7]. The chemical flexibility of this structure makes it a wonderful playground for exploring the effects of chemical pressure and aliovalent substitution. We believe that ZrCuSiAs type oxypnictide materials containing $4d$ or $5d$ transition metals represent an area of potentially rich chemistry and an excellent place to explore for new compositions.

Oxy-phosphide compositions with $4d$ and $5d$ metals such as LnRuPO and LnOsPO have previously been structurally investigated [8,9]. More recently CeRuPO was reported to develop a ferromagnetic (FM) Kondo lattice ground state at low temperature while CeOsPO adopts an anti-ferromagnetic (AFM) state [10]. Cerium is known for having a weak grip on its $4f^1$ electron, which tends to delocalize, giving rise to exchange interactions and long range magnetic ordering of Ce moments mediated via the conduction electrons. Very recently other researchers have demonstrated that CeNi$_{0.8}$Bi$_2$, with a distorted ZrCuSiAs type structure, is a superconductor ($T_c \approx 4$ K) and exhibits light and heavy charge carriers [11]. The cerium free ThCr$_2$Si$_2$ type materials, BaRh$_2$P$_2$ ($T_c \approx 1$ K) and BaIr$_2$P$_2$ ($T_c \approx 2.1$ K), isostructural to BaFe$_2$As$_2$, are also reported to superconduct at low temperature [12].

These examples all highlight the need to further investigate Ce based compositions with the ZrCuSiAs type structure as well as those containing transition metals other than iron.

Previously we have reported on the solid solution LaFe$_{1-x}$Rh$_x$AsO and demonstrated that Rh is an effective dopant for inducing superconductivity in LaFeAsO (max. $T_c \approx 16$ K for $x=$ 0.1) [13]. LaFe$_{1-x}$Ir$_x$AsO compositions have been investigated up to $x \approx 0.3$; however a fully substituted $5d$ ZrCuSiAs type oxy-arsenide has yet to be reported [14]. Here we report the synthesis of CeRhAsO and NdRhAsO, as well as the $5d$ transition metal compositions, LnIrAsO ($Ln=$La, Ce, Nd).

2. Materials and methods

Polycrystalline samples (0.5–1 g) were prepared in an Ar filled glove box using reagents of 3 N (at%) purity or better. Lanthanoid oxides (La$_2$O$_3$, CeO$_2$, Nd$_2$O$_3$) were dehydrated overnight at 850 °C before use, and then reacted directly with lanthanoid metal (-40 mesh or smaller), Rh (or Ir) metal, and As metal. All reagents were finely ground in an agate mortar and pestle, pelletized, and placed in small Al$_2$O$_3$ crucibles, which were then sealed inside evacuated fused silica ampoules ($\approx 1 \times 10^{-4}$ Torr). A typical heating profile was: 20 K h^{-1} to 1273 K for 12–18 h, then down 200 K h^{-1} to room temperature. Resulting products were reground, pressed, and sintered at 1173 K for an additional 12 h to improve density before measuring electronic properties.

Room temperature lattice parameters were determined from powder X-ray diffraction data (PXRD) collected on a Rigaku MiniFlex II from $2\theta=20-90°$ using a step size of 0.02. Copper $K\alpha$ radiation was selected using a graphite monochromator on the diffracted beam. Lattice parameters were obtained through least squares fitting via the software Powder4 [15]. Four-probe resistivity (Cu wires with

Ag epoxy) and magnetic measurements (DC-magnetization, zero field cooled—100 Oe) were done from 3 to 300 K using a Quantum Design Physical Properties Measurement System (PPMS).

3. Results and discussion

The primary phase in all PXRD patterns could be indexed as $P4/nmm$ (#129). Fig. 1 shows the PXRD patterns for the LnIrAsO series; the traces for CeRhAsO and NdRhAsO are similar to the previously reported pattern for LaRhAsO [13]. Secondary phases of Ir and IrAs$_2$ are indicated on the powder X-ray diffraction patterns shown in Fig. 1. The refined lattice parameters for the LnRhAsO and LnIrAsO series are both shown plotted in Fig. 2(a) and lattice parameters along with standard deviations are reported in Table 1. There is a systematic decrease in a and c lattice parameters as smaller lanthanoid cations are substituted and the decrease in cell volume, Fig. 2(b), follows a similar trend as the Fe, Co, and Ru analogs previously reported [16]. The smaller cell volume observed for CeCoAsO was previously rationalized by assuming some Ce to be in a mixed valent state, Ce$^{3+/4+}$. The same rationale may apply to CeRhAsO and CeIrAsO, however further studies will be needed to fully clarify whether mixed valent Ce$^{3+/4+}$ is present.
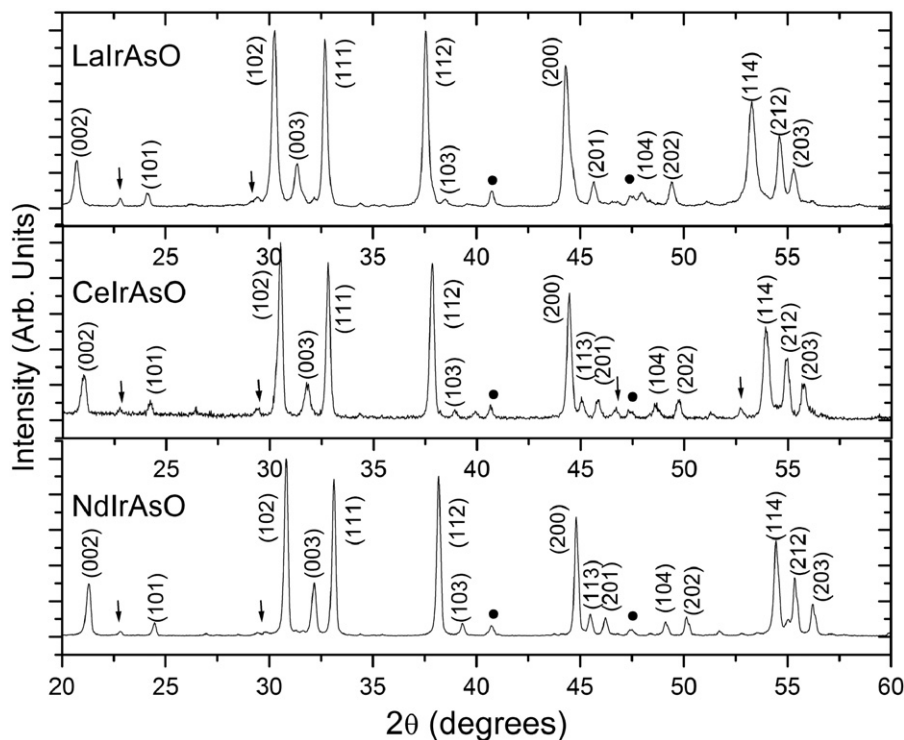

Fig. 1. Room temperature powder X-ray diffraction patterns for the LnIrAsO (Ln=La, Ce, Nd) series. Peaks above 5% relative intensity are labeled with ($h\,k\,l$). Positions of small peaks corresponding to Ir (dots) and IrAs$_2$ (arrows) are indicated.
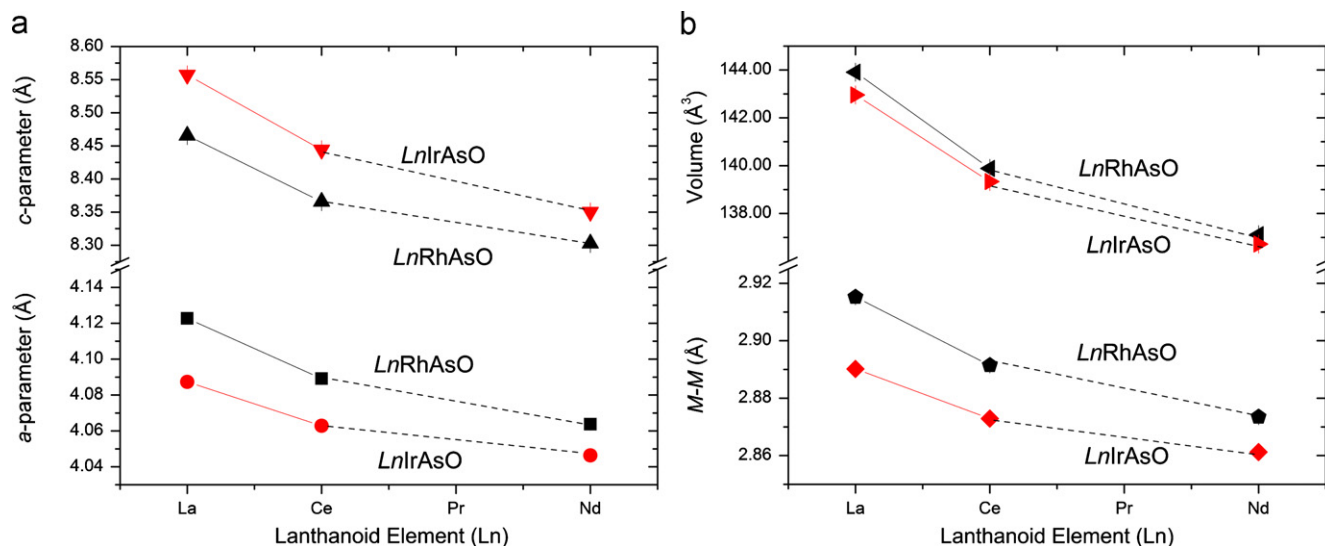

Fig. 2. Lattice parameters for the LnRhAsO and LnIrAsO (Ln=La, Ce, Nd) series (a). Unit cell volume and metal–metal bond distance (M–M) distance for the LnRhAsO and LnIrAsO series (b). * LaRhAsO originally reported in Ref. [13], but shown here for comparison.

What is interesting is that the *a*-parameters observed for *Ln*IrAsO compositions are shorter than the corresponding *Ln*RhAsO compositions. This is somewhat contrary to what might be expected from simple 4*d* and 5*d* orbital size considerations. Take for example the reported lattice parameters of NdCoAsO ($a=3.98$ Å, $c=8.32$ Å) [16], and those found for NdRhAsO ($a=4.064(1)$ Å, $c=8.303(1)$ Å) and NdIrAsO ($a=4.046(1)$ Å, $c=8.350(1)$ Å) as reported in this study. Upon substitution of Rh for Co both the *a*- and *c*-parameters increase, however upon substitution of Ir for Rh the *a*-parameter contracts while the *c*-parameter expands.

The crystal structure for these materials and the square mesh sub-lattice of metal atoms, *M*, within the metal pnictide layer are depicted in Fig. 3(a) and (b), respectively. Often the metal cations are described as having tetrahedral coordination to the pnictide, *Pn*, anions however there are also significant *M–M* interactions at play. This was discussed by Quebe et al., using bond lengths and simple electron counting for *Ln*FeAsO materials and later evidenced through band structure calculations of LaFeAsO [16,17]. The metal–metal (*M–M*) bond distances in *Ln*MAsO materials are reflected in the unit cell *a*-parameter as $a=\sqrt{2}(M\text{–}M)$ and the decrease in *a*-parameter therefore means the Ir–Ir bond is shorter than the Rh–Rh bond formed in these materials, Fig. 2(b). The Ir–Ir bond length observed for NdIrAsO is about 5.2% longer than that of Ir metal while the Rh–Rh bond length in NdRhAsO is about 6.4% longer than for Rh metal [18,19]. Presumably the decrease in the *M–M* bond length is accompanied by an increase in the *c*-parameter as pnictide anions move toward the rare earth atoms, expanding the width of the M_2As_2 layer. Further crystal structure refinements in conjunction with electronic structure calculations are in progress to better understand how the *M–M* and *M–Pn* interactions change upon substituting for a 5*d* metal; however, the best explanation for the decrease in *a* parameter may simply be that the increased size of the Ir 5*d* orbitals enhances bonding type interactions between partially filled metal *d*-orbitals.

All *Ln*RhAsO and *Ln*IrAsO compositions are metallic; normalized resistivity is shown in Fig. 4(a) and (b). Immediately clear are the precipitous drops in resistivity beginning at 7 K for CeRhAsO and 10 K for CeIrAsO. Fig. 5(a) and (b) highlight the low temperature regions around these transitions. It can be seen from the low temperature plot of CeIrAsO that by 3 K, the lowest temperature measured in this study, the resistivity appears to be leveling out and is no longer dropping. One cause for the sudden drop in resistivity could be reduced carrier scattering, due to long range magnetic ordering of the Ce^{3+} $4f^1$ electrons. This has been observed for CeFeAsO and PrFeAsO compositions, the latter of which

Table 1
Lattice parameters for *Ln*RhAsO and *Ln*IrAsO compounds.

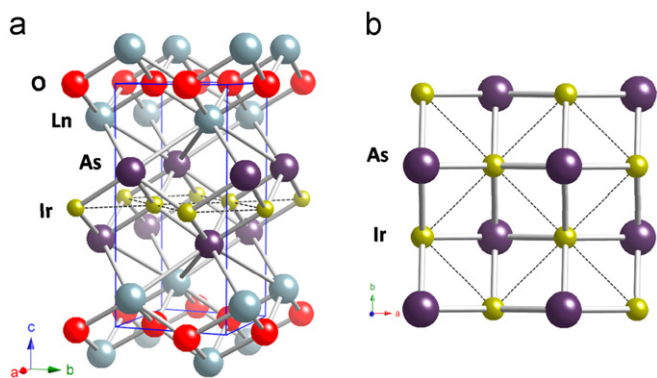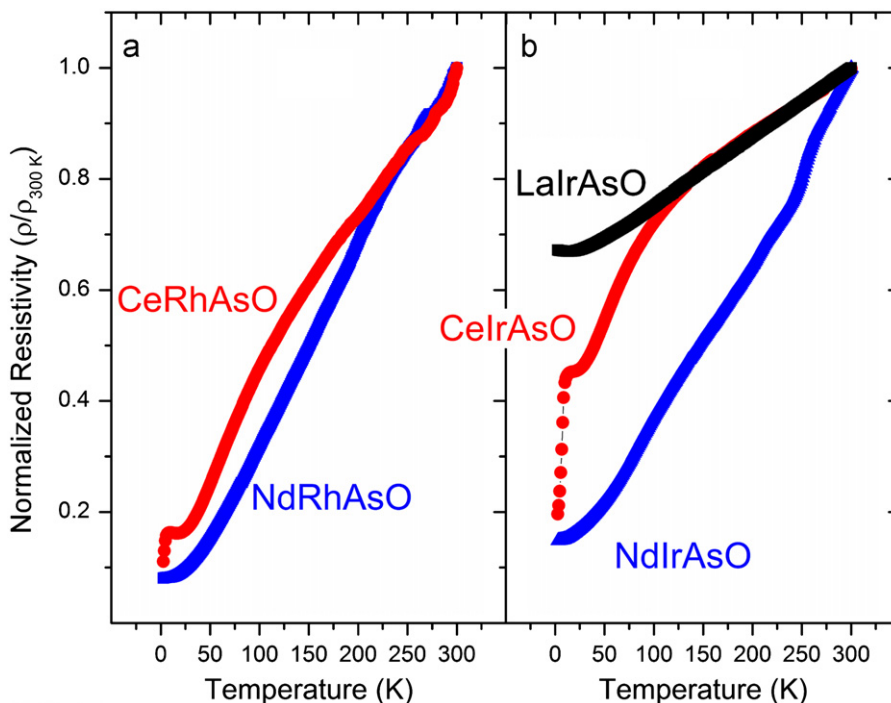| Compound	*a*-parameter	*c*-parameter
CeRhAsO	4.089(1)	8.365(2)
NdRhAsO	4.063(1)	8.303(1)
LaIrAsO	4.087(1)	8.557(1)
CeIrAsO	4.063(1)	8.444(2)
NdIrAsO	4.046(1)	8.350(1)

Fig. 3. Crystal structure of *Ln*MAsO (*Ln*=La, Ce, Nd and *M*=Rh, Ir) compositions (a). View of the metal pnictide layer along the *c*-axis with dashed lines highlighting the *M–M* bond distance (b).

Fig. 4. Normalized resistivity ($\rho/\rho_{300\ K}$) for *Ln*RhAsO (*Ln*=Ce, Nd) (a) and *Ln*IrAsO (*Ln*=La, Ce, Nd) compositions (b).
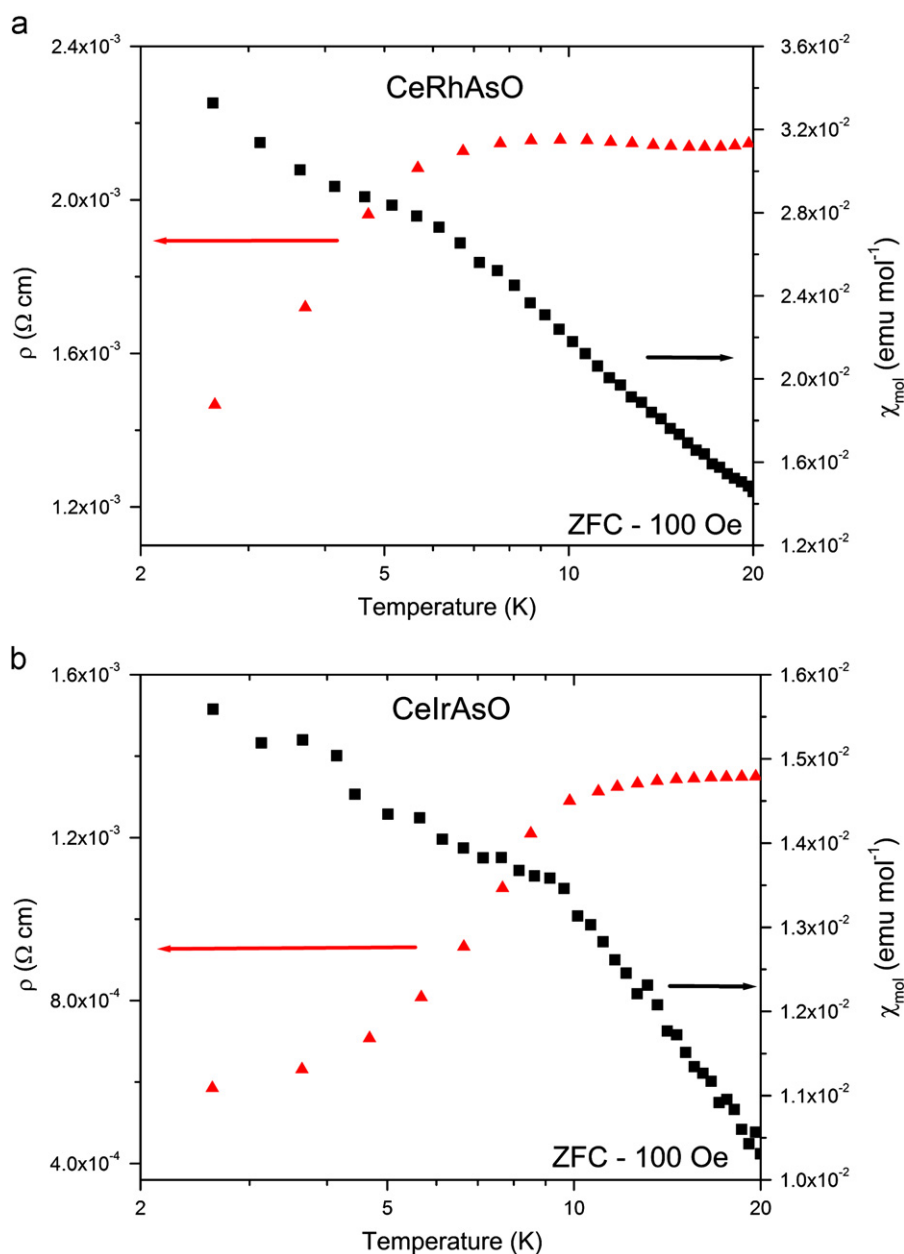
Fig. 5. Low temperature resistivity for CeRhAsO (a) and CeIrAsO (b) compositions overlaid with zero field cooled (ZFC) molar magnetic susceptibility measurements at 100 Oe applied field.

demonstrated a sudden step down in resistivity at 13 K coinciding with a small change in the magnetization [20]. Similar temperature dependence of resistivity has been reported for CeNiAsO, including a low temperature resistivity drop at around 9.3 K [21]. A very recent preprint has appeared which proposes that this occurs from AFM ordering of the Ce moments and that CeNiAsO is a AFM Kondo lattice material with strong hybridization between 4f and 3d electrons [22]. Overlaid with the low temperature resistivity for CeRhAsO and CeIrAsO in Fig. 5(a) and (b) is the molar susceptibility as measured through the transition region. From these plots it can be seen that there is a slight change in the magnetization corresponding to the resistivity transition temperature. It should be noted however that the measured magnetization for the CeIrAsO composition in the low temperature region is only one order of magnitude above the sensitivity limit of the PPMS, causing noticeable noise in the collected data. Nevertheless the slight change in magnetization for CeRhAsO

and CeIrAsO samples correlate well with the resistivity changes observed and this indicates that the origin of the resistivity drop for these compositions is most likely connected to a magnetic transition similar to that of CeNiAsO [22]. Given that the observed properties only occur for the Ce compositions within each series it could also be inferred that the root cause of the transition must be interactions between transition metal d-orbitals and Ce $4f^1$ electrons.

It is interesting to note the cell parameters and resistivity transitions observed for CeRhAsO ($a=4.089(1)$ Å, $c=8.366(2)$ Å, $T=7$ K), CeIrAsO ($a=4.063(1)$ Å, $c=8.444(2)$ Å, $T=10$ K), and those recently reported for CeNiAsO ($a=4.077$ Å, $c=8.102$ Å, $T_N=9.3$ K) [22]. It can be seen that the material with the shortest M–M bond distance demonstrates the highest temperature of transition. The composition CeRuAsO ($a=4.096$ Å, $c=8.380$ Å), which has larger lattice parameters than CeRhAsO, does not show a transition above 3 K [16]. There is no apparent correlation to the c-parameter length

however, i.e. CeRhAsO and CeIrAsO are both substantially longer than CeNiAsO; however the observed transition for CeRhAsO is at a lower temperature. More sensitive magnetism measurements as well as complimentary transport studies, such as thermopower and specific heat, of CeRhAsO and CeIrAsO are warranted given the interesting low temperature electronic behavior observed. If property origins of CeRhAsO and CeIrAsO are indeed similar to CeNiAsO then solid solutions between these materials may provide a knob by which to tune exchange interactions and thereby explore Kondo lattice related phenomena.

4. Conclusion

New layered oxyarsenides containing the $4d$ and $5d$ metals Rh and Ir have been synthesized. Compositions from the series LnRhAsO and LnIrAsO show systematic decrease in lattice parameters and unit cell volumes as the rare earth ionic radius decreases. Upon substitution of Ir for Rh the a-parameter decreases which results in a shorter $M–M$ interaction within the metal pnictide layer. CeRhAsO and CeIrAsO show a strong deviation from La and Nd based compositions in their temperature dependence of resistivity, with each showing a sudden drop in resistivity at 7 and 10 K, respectively. This behavior is very similar to that reported for CeNiAsO, an AFM Kondo lattice material, but only a slight change in magnetization has been observed thus far for CeRhAsO and CeIrAsO at the resistivity transition temperature. Metallic cerium based compositions have long been known to demonstrate interesting properties related to the interplay of their $4f^1$ electrons with the conduction band electrons. Cerium based oxypnictide compounds are therefore structurally and compositionally related to many exciting areas of science. While further investigations of CeRhAsO and CeIrAsO will be needed to pinpoint the exact origins of their structural changes and transport behavior, the findings presented demonstrate that exciting new ZrCuSiAs type compounds are still waiting to be explored.

References

[1] Y. Kamihara, T. Watanabe, M. Hirano, H. Hosono, J. Am. Chem. Soc. 130 (2008) 3296–3297.
[2] Z.-A. Ren, J. Yang, W. Lu, W. Yi, G.-C. Che, X.-L. Dong, L.-L. Sun, Z.-X. Zhao, Mater. Res. Innov. 12 (2008) 105–106.
[3] Z.-A. Ren, W. Lu, J. Yang, W. Yi, X.-L. Shen, Z.-C. Li, G.-C. Che, X.-L. Dong, L.-L. Sun, F. Zhou, Z.-X. Zhao, Chin. Phys. Lett. 25 (2008) 2215–2216.
[4] M. Rotter, M. Tegel, D. Johrendt, Phys. Rev. Lett. 101 (2008) 107006–4.
[5] F.-C. Hsu, J.-Y. Luo, K.-W. Yeh, T.-K. Chen, T.-W. Huang, P.M. Wu, Y.-C. Lee, Y.-L. Huang, Y.-Y. Chu, D.-C. Yan, M.-K. Wu, Proc. Natl. Acad. Sci. USA 105 (2008) 14262–14264.
[6] X.C. Wang, Q.Q. Liu, Y.X. Lv, W.B. Gao, L.X. Yang, R.C. Yu, F.Y. Li, C.Q. Jin, Solid State Commun. 148 (2008) 538–540.
[7] R. Pöttgen, D. Johrendt, Z. Naturforsch. 63b (2008) 1135–1148.
[8] B.I. Zimmer, W. Jeitschko, J.H. Albering, R. Glaum, M. Reehuis, J. Alloys Compd. 229 (1995) 238–242.
[9] W. Jeitschko, B.I. Zimmer, R. Glaum, L. Boonk, U.C. Rodewald, Z. Naturforsch. 63b (2008) 934–940.
[10] C. Krellner, N.S. Kini, E.M. Bruning, K. Koch, H. Rosner, M. Nicklas, M. Baenitz, C. Geibel, Phys. Rev. B 76 (2007) 104418.
[11] H. Mizoguchi, S. Matsuishi, M. Hirano, M. Tachibana, E. Takayama-Muromachi, H. Kawaji, H. Hosono, Phys. Rev. Lett. 106 (2011) 057002.
[12] D. Hirai, T. Takayama, R. Higashinaka, H. Aruga-Katori, H. Takagi, J. Phys. Soc. Jpn. 78 (2009) 023706.
[13] S. Muir, A.W. Sleight, M.A. Subramanian, Mater. Res. Bull. 45 (2010) 392–395.
[14] Y. Qi, L. Wang, Z. Gao, D. Wang, X. Zhang, Z. Zhang, Y. Ma, Phys. Rev. B 80 (2009) 054502.
[15] N. Dragoe, J. Appl. Crystallogr. 34 (2001) 535.
[16] P. Quebe, L.J. Terbüchte, W. Jeitschko, J. Alloys Compd. 302 (2000) 70–74.
[17] D.J. Singh, M.H. Du, Phys. Rev. Lett. 100 (2008) 237003–237004.
[18] H.E. Swanson, G.M. Ugrinic, Nat. Bur. Stand (U.S.) Circ. 3 (1954) 1–75.
[19] H.E. Swanson, G.M. Ugrinic, Nat. Bur. Stand (U.S.) Circ. 5 (1955) 1–75.
[20] M.A. McGuire, R.P. Hermann, A.S. Sefat, B.C. Sales, R. Jin, D. Mandrus, F. Grandjean, G.J. Long, New J. Phys. 11 (2009) 025011.
[21] C. Gen-Fu, L. Zheng, W. Dan, D. Jing, L. Gang, H. Wan-Zheng, Z. Ping, L. Jian-Lin, W. Nan-Lin, Chin. Phys. Lett. 25 (2008) 2235–2238.
[22] Y. Luo, H. Han, H. Tan, X. Lin, Y. Li, S. Jiang, C. Feng, J. Dai, G. Cao, Z. Xu, S. Li, http://arxiv.org (2011) arXiv1103.3073.